Toward real-time high-fidelity simulation using integral boundary layer modeling

By A. Marques, Q. Wang†, J. Larsson‡, G. Laskowski¶ AND S. T. Bose‖

One of the greatest challenges to using large-eddy simulations (LES) in engineering applications is the large number of grid points required near walls. To mitigate this issue, researchers often couple LES with a simplified model of the flow close to the wall, known as the wall model. One feature common to most wall models is that the first few (about 3) grid points must be located below the inviscid log-layer ($y/\delta < 0.2$), and the grid must have near-isotropic resolution near the wall. Hence, wall-modeled LES may still require a large number of grid points in both the wall-normal and span-wise directions. Because of these requirements, wall-modeled LES is still unfeasible in many applications. We present a new formulation of wall-modeled LES that is being developed to address this issue. In this formulation, LES is used to solve only for the features of the velocity field that can be adequately represented on the LES grid. The effects of the unresolved features are captured by imposing an integral balance of kinetic energy in the near-wall region. This integral energy balance translates into a dynamic partial differential equation defined on the walls, which is coupled to the LES equations. We discuss details of the new formulation and present results obtained in laminar channel flows.

1. Introduction

One of the greatest challenges of using LES in engineering applications is the large number of grid points required to resolve the small scales related to viscous effects near solid walls. To mitigate this issue, researchers often couple LES with a simplified model of the flow close to the wall, known as the wall model (Piomelli & Balaras 2002; Sagaut 2006; Kawai & Larsson 2010). One feature common to most wall models is that the first few (about 3) grid points must be located below the inviscid log-layer ($y/\delta < 0.2$), and the grid must have near-isotropic resolution near the wall. Hence, wall-modeled LES may require a large number of grid points in both the wall-normal and span-wise directions. Because of these requirements, wall-modeled LES is still unfeasible in many applications.

We are developing a new formulation of wall-modeled, time-filtered LES to address this issue. While the formulation is aimed at turbulent flows, so far the development has been restricted to laminar channel flows. In certain configurations, the dynamic evolution of laminar channel flows results in very large velocity gradients. These large gradients are due to viscous effects restricted to the near-wall region, and depend mostly on the localized features of the flow, which are amenable models that are relatively independent of specific applications. These are the same kinds of models that we intend to develop for turbulent flows. Furthermore, the relative simplicity of laminar channel flows allows us to create and test models with low computational cost in this initial stage of development.

† Department of Aeronautics and Astronautics, Massachusetts Institute of Technology
‡ Department of Mechanical Engineering, University of Maryland
¶ GE Aviation
‖ Cascade Technologies Inc.

The new wall model formulation is based on the decomposition of the velocity field (time-filtered in the turbulent case) into two components

$$\vec{q} = \vec{q}_{\mathrm{ow}} + \vec{q}_{\mathrm{nwd}}. \tag{1.1}$$

The off-wall component ($\vec{q}_{\mathrm{ow}}$) includes only the large flow scales prevalent away from the wall, whereas the near-wall defect component $\vec{q}_{\mathrm{nwd}}$ takes into account the small near-wall scales not included in the off-wall component. In performing this decomposition we operate under the assumption that, at least away from solid walls, the long time scales are associated with large spatial scales, and we use a finite volume discretization on a relatively coarse grid to compute the off-wall component. Note that there is no grid resolution error incurred in this step, since the off-wall component includes only scales that can be resolved by the coarse grid.

We supplement the governing equations of the off-wall component with data-driven models of the effects of the unresolved small scales near the wall. We build these models based on relationships measured on numerical data obtained in fully resolved simulations. Furthermore, these models are parametrized by a low-dimensional feature space that depends only on localized integral flow quantities. Hence, we solve only for the integral quantities of the near-wall defect component that affect the governing equations of the off-wall component. As discussed in Section 3, in the case of laminar channel flows it is sufficient to augment the system with the integral balance of kinetic energy in the first grid cell above the wall. This approach is conceptually similar to the classical integral boundary layer formulation used to model viscous effects coupled with inviscid flow formulations (Drela & Giles 1987).

The remainder of this report is organized as follows. In Section 2 we discuss the laminar channel flows that are the subject of the current investigation. We present in detail the new wall model formulation in Section 3 and show preliminary results in Section 4. In Section 5 we list the steps needed to advance the development of the formulation, and in Section 6 we make final remarks.

2. Laminar channel flow

The present investigation was primarily based on laminar channel flows. The combination of periodicity and lack of turbulence reduces the formulation of such flows to a simple one-dimensional heat equation, given by

$$\frac{\partial u}{\partial t} - \nu \frac{\partial^2 u}{\partial y^2} = -\frac{1}{\rho}\frac{dp}{dx}, \tag{2.1}$$

where dp/dx denotes the constant pressure gradient that drives the flow. Despite the simplicity of Eq. (2.1), this model problem includes the viscous dissipation effects that dominate the dynamics in the near-wall region.

In certain circumstances, Eq. (2.1) can lead to the development of viscous boundary layers with very large velocity gradients. In principle, resolving these large gradients requires very fine grids. The objective of the present investigation is to create a wall model formulation that allows the solution of such flows with relatively coarse grids, such that these gradients are under-resolved or not resolved at all. Furthermore, we want to develop a formulation that can be extended to more complex physics, including turbulent flows.

One situation in which Eq. (2.1) can lead to large velocity gradients is illustrated in

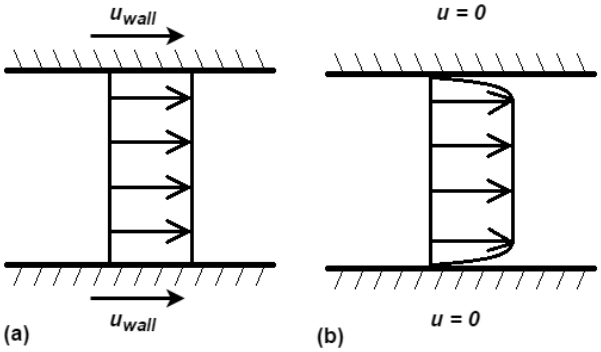

FIGURE 1. Prototype laminar channel flow problem with large velocity gradient. (a) Flow is initially uniform moving along with wall. (b) Immediately after the wall stops large velocity gradients develop in the near-wall region.

Figure 1. This figure depicts the situation in which, initially, the channel walls are moving with a constant speed u_{wall}, and the channel flow is uniform with the same speed as the walls. In this setting, the flow is completely driven by the motion of the walls, and there is no pressure gradient along the channel. Then, the walls are brought to a sudden stop. In the moments that follow the stopping of the walls, the flow immediately adjacent to the wall is forced to stop due to friction, whereas the flow at the bulk of the channel continues to move at a speed close to u_{wall}. This situation results in very large velocity gradients in the wall-normal direction. We use this prototype flow to assess the performance of our wall model formulation.

3. Formulation

In practice, the velocity decomposition in Eq. (1.1) is obtained by defining the off-wall velocity component. The near-wall defect component follows from the difference between the off-wall and the (unknown) complete velocity fields. Our experience showed that an effective way to define the off-wall velocity component is to apply a spatial filter to the complete velocity field. By judiciously selecting the spatial filter, we can always guarantee that the off-wall component can be adequately represented in a relatively coarse grid.

As mentioned above, the present investigation is restricted to laminar channel flows. However, in the case of turbulent flows we expect the effect of the spatial filter on the already time-filtered velocity to be restricted to the near-wall region. This follows from the assumption that, away from the wall, the long time scales are related to large spatial scales. We will examine the validity of this assumption in future work.

In this investigation we adopted the grid cell averaging as the spatial filter, a common approach in LES formulations (Moin *et al.* 1991; Sagaut 2006; You & Moin 2007). The filtered velocity at the i-th cell is given by

$$\langle u \rangle_i = \frac{1}{V_i} \int_{V_i} u \, dV, \tag{3.1}$$

where V_i denotes the volume of the i-th cell. When applied to a fine grid, the filtered velocity satisfies the standard finite volume discretization of the governing equations. On the other hand, when applied to a coarse grid, the fluxes between grid cells in the near-wall region depend on small-scale features that are not resolved in the off-wall

velocity component. Hence, standard approximations used to compute the fluxes between grid cells are not accurate in the near-wall region, and we must supplement the finite volume discretization with more accurate flux estimates. Furthermore, these estimates must be based on relationships between these small-scale features and the large-scale features resolved in the coarse grid. These relationships can be measured in fully resolved simulations.

In the case of laminar channel flows, the finite volume discretization of Eq. (2.1) results in

$$\frac{d\langle u\rangle_i}{dt} - \frac{F_{i+1/2} - F_{i-1/2}}{\Delta y_i} = -\frac{1}{\rho}\frac{dp}{dx}, \tag{3.2}$$

where Δy_i is the length of the i-th grid cell and F denotes the momentum flux between grid cells. For grid cells away from the wall, F is approximated by

$$F_{i+1/2} = \frac{2\nu(\langle u\rangle_{i+1} - \langle u\rangle_i)}{\Delta y_{i+1} + \Delta y_i}. \tag{3.3}$$

In the current investigation we supplement the finite volume discretization with models for the skin friction coefficient and the momentum flux between the first and second cells, given by

$$C_{f_0} = \frac{\nu}{0.5u_r^2}\left.\frac{\partial u}{\partial y}\right|_{y=0}, \tag{3.4}$$

$$C_{f_1} = \frac{\nu}{0.5u_r^2}\left.\frac{\partial u}{\partial y}\right|_{y=\Delta y_1}, \tag{3.5}$$

where

$$u_r = \sqrt{\langle u\rangle_1 + \langle u\rangle_2} \tag{3.6}$$

is a reference velocity scale. We parametrized these models using an approach analogous to the one used in the classical integral boundary layer formulation (Drela & Giles 1987). Namely, we define quantities analogous to the displacement (δ^*) and momentum thicknesses (θ) as follows

$$\delta^* = \left(1 - \frac{\langle u\rangle_1}{u_r}\right)\Delta y_1, \tag{3.7}$$

$$\theta = \left(\frac{\langle u\rangle_1}{u_r} - \frac{\langle u^2\rangle_1}{u_r^2}\right)\Delta y_1. \tag{3.8}$$

We then normalize the quantities of interest with respect to θ and u_r and measure the following relationships

$$\mathrm{Re}_\theta C_{f_0} = \mathrm{Re}_\theta C_{f_0}(H), \qquad \mathrm{Re}_\theta C_{f_1} = \mathrm{Re}_\theta C_{f_1}(H), \tag{3.9}$$

where $H = \delta^*/\theta$ is the shape factor, and $\mathrm{Re}_\theta = u_r\theta/\nu$ denotes the Reynolds number with respect to θ.

Figures 2 and 3 show the values of $\mathrm{Re}_\theta C_{f_0}$ and $\mathrm{Re}_\theta C_{f_1}$ as a function of the shape factor. These values are based on a solution of Eq. (2.1) with a fine grid with 1,025 nodes. Furthermore, C_{f_1} is measured between the first and second grid cells of a coarse grid. Figure 3 shows $\mathrm{Re}_\theta C_{f_1}$ for several values of coarse grid spacing. Nevertheless, after the normalization all curves nearly collapse. The exception is $\Delta y = 0.5L$ at higher values of H.

Equations (3.2)-(3.9) do not result in a closed system. Namely, Eq. (3.8) depends on

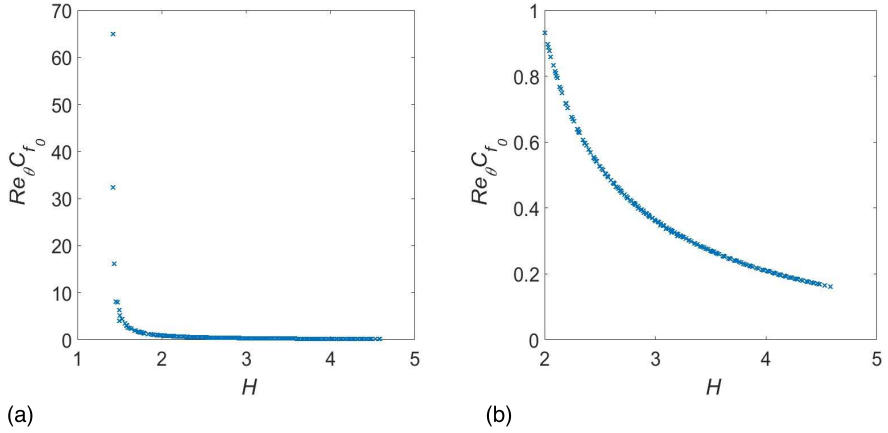

FIGURE 2. Skin friction coefficient, normalized by u_r and θ, as a function of the shape factor H. (a) Full range of H. (b) Enlarged view of the range $H > 2$.

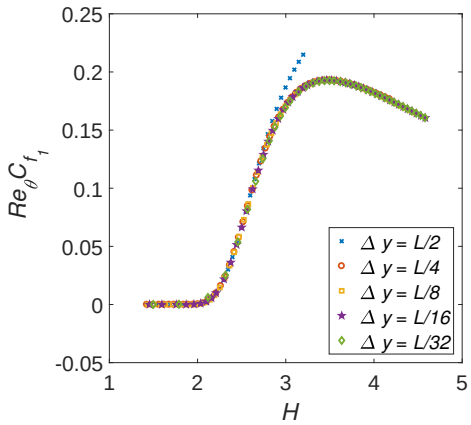

FIGURE 3. Momentum flux between first and second grid cells, normalized by u_r and θ as a function of the shape factor H. Results for several values of the wall-normal grid spacing, as a fraction of the channel width L.

$\langle u^2 \rangle_1$, related to the cell average of kinetic energy in the first grid cell, and is not readily available as a solution of Eq. (3.2). We solve for $\langle u^2 \rangle_1$ by augmenting Eq. (3.2) with an integral balance of kinetic energy at the first grid cell. Namely, the evolution $\langle u^2 \rangle_1$ is obtained by multiplying Eq. (2.1) by u and computing the average over the first grid cell, as follows

$$\frac{d\langle u^2 \rangle_1}{dt} - u_r^3 C_D = -\frac{1}{\rho}\frac{dp}{dx}\langle u \rangle_1, \tag{3.10}$$

where

$$C_D = \frac{\nu}{0.5 u_r^3}\int_0^{\Delta y_1} u \frac{\partial^2 u}{\partial y^2}\, dy \tag{3.11}$$

is the viscous dissipation coefficient. We can also rewrite Eqs. (3.2)-(3.10) in terms of the

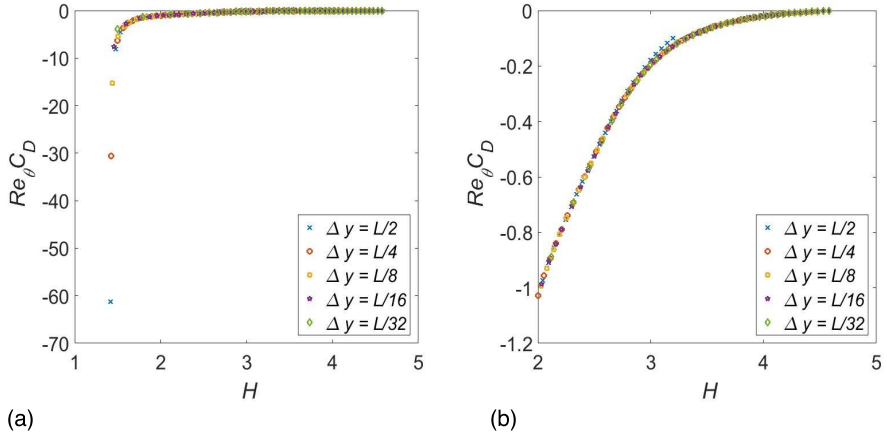

FIGURE 4. Viscous dissipation in the first grid cell, parametrized by the shape factor H. (a) Full range of H. (b) Enlarged view of range $H > 2$.

evolution of the shape factor H as follows,

$$\frac{1}{\mathrm{Re}_\theta}\frac{dH}{dt} - \frac{2HC_D}{\theta^2} + 2H(C_{f_1} - C_{f_0})\left[\frac{2}{\theta^2} - \frac{2H}{\Delta y_1 \theta} + \frac{H(H+1)}{\Delta y_1^2}\right] - 2\frac{\langle u\rangle_2}{u_r}(\bar{C}_{f_2} - C_{f_1})\left[\frac{H(H+1)\theta + \Delta y_1(1-H)}{\Delta y_2 \theta^2}\right] = -\frac{\nu}{\theta \rho u_r^2}\frac{dp}{dx}\left[H(H+1)\left(\frac{\langle u\rangle_2}{u_r} - \frac{H^2\theta}{\Delta y_1}\right) + (1-H)\frac{\langle u\rangle_2}{u_r}\frac{\Delta y_1}{\theta}\right], \quad (3.12)$$

where

$$\bar{C}_{f_2} = \frac{\nu F_{2.5}}{0.5 u_r^2}. \quad (3.13)$$

Finally, the viscous dissipation coefficient C_D also needs to be modeled as a function of the shape factor, after proper normalization. Figure 4 shows $\mathrm{Re}_\theta C_D$ as a function of the shape factor for several values of coarse grid spacing. This figure shows that, after appropriate normalization, the results for C_D also nearly collapse into a single curve.

The formulation described above can be interpreted as a coupled system of governing equations for the off-wall velocity component and an integral feature that depends on the near-wall defect (cell-averaged kinetic energy). The near-wall defect component affects the off-wall equations in two ways: (i) a Neumann boundary condition in the form of a prescribed shear stress at the wall, and (ii) additional volumetric source terms that model the momentum flux between neighboring grid cells in the near-wall region (here we restricted the effect of this source term to the first two grid cells). On the other hand, the off-wall component affects the governing equation of the near-wall component in the form of source terms in Eq. (3.12).

4. Results

We verified the validity of the formulation discussed in Section 3 in a series of test cases involving laminar channel flows in which the walls are brought to a sudden stop, as described in Section 2. Figure 5 shows snapshots of the off-wall velocity component at

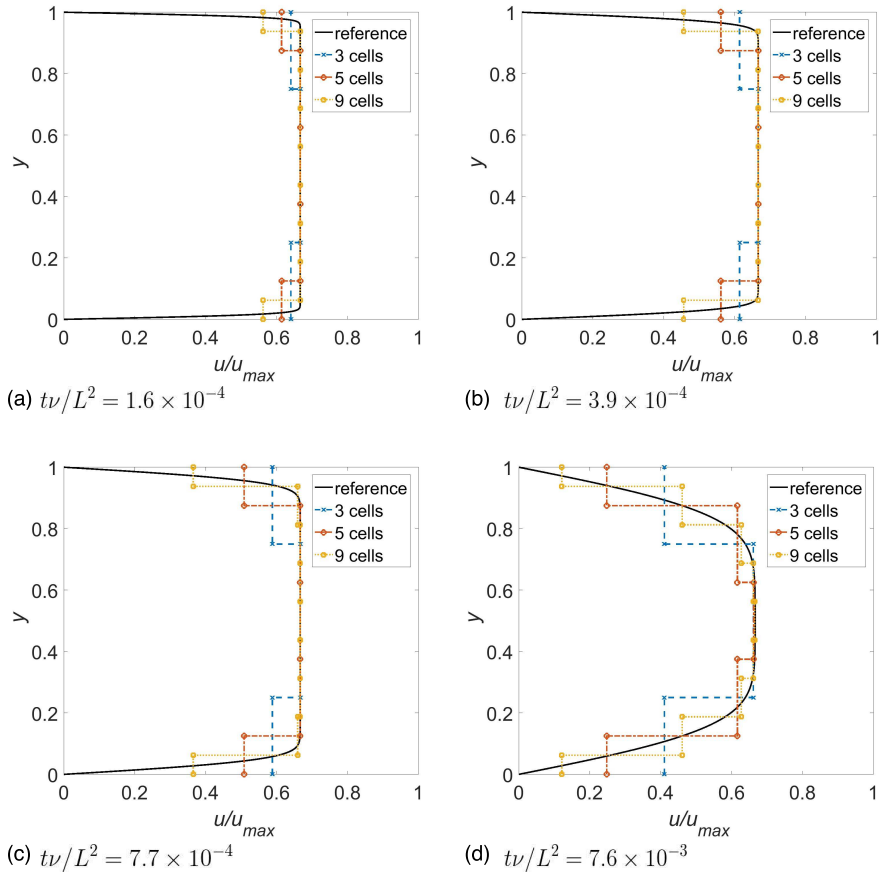

FIGURE 5. Solution of a laminar channel flow brought to a sudden stop. Comparison between a refined solution (1,025 nodes) and solutions obtained with the new wall model at (a) $t\nu/L^2 = 1.6 \times 10^{-4}$, (b) $t\nu/L^2 = 3.9 \times 10^{-4}$, (c) $t\nu/L^2 = 7.7 \times 10^{-4}$, and (d) $t\nu/L^2 = 7.6 \times 10^{-3}$.

different moments in time. We can visually inspect that the off-wall velocity component is close to the reference solution averaged over the grid cells. Furthermore, Figures 6 and 7 show comparisons of $\langle u \rangle_1$ and $\langle u^2 \rangle_1$ computed with the new formulation and values computed directly from the reference solution. We can observe that the current formulation produces accurate results in the initial development of the boundary layer, when large velocity gradients are observed.

5. Next steps

The formulation presented in Section 3 proved successful to compute solutions of laminar channel flows even when large velocity gradients are grossly under-resolved. However, preliminary results (not shown here) indicate that simulations may present instabilities if time integration is carried out long enough. It is paramount that we determine whether this behavior stems from numerical instabilities that can be remedied, or from accrual of errors from the models used to supplement the cell-averaged equations.

Furthermore, so far we restricted our attention to the model problem of laminar channel

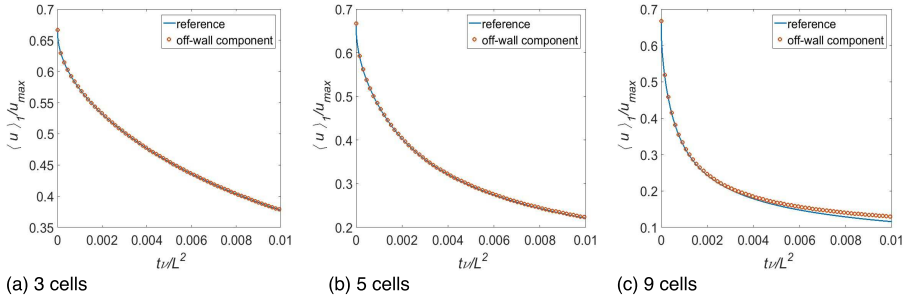

FIGURE 6. Cell average velocity at the first grid cell. Comparison between solutions obtained with the new wall model formulation with coarse grids – (a) 3, (b) 5, and (c) 9 grid cells – and values computed directly from a reference solution obtained with 1,025 grid nodes.

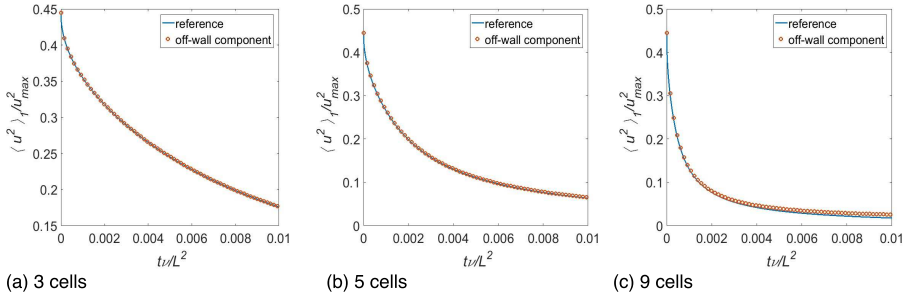

FIGURE 7. Cell average kinetic energy at the first grid cell. Comparison between solutions obtained with the new wall model formulation with coarse grids – (a) 3, (b) 5, and (c) 9 grid cells – and values computed directly from a reference solution obtained with 1,025 grid nodes.

flows. However, the goal of this research is to develop effective wall models for simulating turbulent flows. Hence, the natural extension of this work is to apply an analysis similar to the one presented in Section 3 to channel flows in the turbulent regime. The challenge in this development lies in the fact that, contrary to the simple model problem studied in this work, the near-wall dynamics of turbulent flows are not restricted to one-dimensional viscous effects. Hence, additional terms are needed to supplement the cell-averaged governing equations. In addition, these terms may potentially depend on a higher-dimensional feature space that has yet to be identified.

Finally, due to the chaotic nature of turbulent flows, we anticipate that relationships such as the ones shown in Figures 2-4 will not collapse so tightly as observed in the laminar regime. In this situation, we foresee the application of supervised learning techniques to create the models needed to supplement the cell-averaged governing equations. This approach can create models based on the large amounts of DNS data available for turbulent channel flows (Perlman *et al.* 2007; Li *et al.* 2008; Graham *et al.* 2003), and results in stochastic models that allows us to quantify the model inadequacy related to the use of wall models in turbulent simulations. A similar technique has been applied in the context of the classical integral boundary layer formulation (Marques *et al.* 2016).

6. Conclusions

We developed a new wall model formulation for laminar channel flows that produced accurate results even when large velocity gradients are grossly under-resolved. This work constitutes the initial stage in the development of wall models for LES simulations of turbulent flows that are nearly independent of the Reynolds number.

The formulation developed here is based on a decomposition of the velocity field into (i) the cell average (off-wall component) and (ii) the defect between the cell average and the complete velocity (near-wall defect component). The cell average quantities are computed with a finite volume discretization of the governing equations, supplemented with models for the shear stress and viscous dissipation in the near-wall region. These models represent the effect of the defect component on the cell averages, and work effectively as boundary conditions and additional source terms applied to the finite volume discretization.

Furthermore, these models for shear stress and viscous dissipation in the near-wall region are created based on numerical data obtained from fully resolved simulations. In the case of laminar channel flows, it was possible to parametrize this information with a single parameter, which is analogous to the shape factor defined in classical boundary layer theory.

We are currently working to extend the formulation discussed here to solve turbulent flows in situations in which geometrically thin boundary layers are under-resolved or not resolved at all. We believe that the combination of a formal velocity decomposition and data-driven models of the defect terms has the potential to produce accurate wall models in such situations, and results in a wall-modeled LES formulation that meets the cost and accuracy demands of practical engineering applications.

Acknowledgments

The authors are grateful to the many participants of the CTR summer program who engaged in thoughtful discussions about this project, especially Prof. Peter Schmid.

REFERENCES

Drela, M. & Giles, M. B. 1987 Viscous-inviscid analysis of transonic and low Reynolds number airfoils. *AIAA J.* **25**, 1347–1355.

Graham, J., Lee, M., Malaya, N., Moser, R., Eyink, G., Meneveau, C., Kanov, K., Burns, R. & Szalay, A. 2013 *Turbulent channel flow data set*. http://turbulence.pha.jhu.edu/docs/README-CHANNEL.pdf.

Kawai, S. & Larsson, J. 2010 A dynamic wall model for large-eddy simulation of high Reynolds number compressible flows. *Annual Research Briefs*, Center for Turbulence Research, Stanford University, pp. 25-37.

Li, Y., Perlman, E., Wan, M., Yang, Y., Burns, R., Meneveau, C., Burns, R., Chen, S., Szalay, A. & Eyink, G. 2008 A public turbulence database cluster and applications to study Lagrangian evolution of velocity increments in turbulence. *J. Turbul.* **9**, 1–29.

Marques, A., Wang, Q. & Marzouk, Y. 2016 Data-driven probabilistic boundary layer modeling for airfoil performance prediction. *AIAA Paper* 2016–3864.

Moin, P., Squires, K., Cabot, W. & Lee, S. 1991 A dynamic subgrid-scale model for compressible turbulence and scalar transport. *Phys. Fluids.* **3**, 2746-2757.

Perlman, E., Burns, R., Li, Y. & Meneveau, C. 2007 Data exploration of turbulence

simulations using a database cluster. *Proceedings of the 2007 ACM/IEEE Conference on Supercomputing*, pp. 23:1–23:11.

Piomelli, U. & Balaras, E. 2002 Wall-layer models for large-eddy simulations. *Annu. Rev. Fluid Mech.* **34**, 349–374.

Sagaut, P. 2006 *Large Eddy Simulation for Incompressible Flows: An Introduction*. Springer Science & Business Media.

You, D. & Moin, P. 2007 A dynamic global-coefficient subgrid-scale model for large-eddy simulation of turbulent scalar transport in complex geometries Local energy transfer and nonlocal interactions in homogeneous, isotropic turbulence. *Proceedings of the Summer Program,* Center for Turbulence Research, Stanford University, pp. 169–182.